Volume 56(1): 3–6, 2008
Journal of Histochemistry & Cytochemistry
http://www.jhc.org

ARTICLE

Evidence That the ZNT3 Protein Controls the Total Amount of Elemental Zinc in Synaptic Vesicles

David H. Linkous, Jane M. Flinn, Jae Y. Koh, Antonio Lanzirotti, Paul M. Bertsch, Blair F. Jones, Leonard J. Giblin, and Christopher J. Frederickson

Department of Psychology, George Mason University, Fairfax, Virginia (DHL,JMF); Department of Neurology, University of Ulsan College of Medicine, Poongnapdong, Songpagu, Seoul, South Korea (JYK); Consortium for Advanced Radiation Sources, University of Chicago, Chicago, Illinois (AL); National Synchrotron Light Source, Brookhaven National Laboratory, Upton, New York (AL); Savannah River Ecology Laboratory, University of Georgia, Aiken, South Carolina (PMB); United States Geological Survey, Reston, Virginia (BFJ); and NeuroBioTex, Inc., Galveston, Texas (LJG,CJF)

SUMMARY The ZNT3 protein decorates the presynaptic vesicles of central neurons harboring vesicular zinc, and deletion of this protein removes staining for zinc. However, it has been unclear whether only histochemically reactive zinc is lacking or if, indeed, total elemental zinc is missing from neurons lacking the *Slc30a3* gene, which encodes the ZNT3 protein. The limitations of conventional histochemical procedures have contributed to this enigma. However, a novel technique, microprobe synchrotron X-ray fluorescence, reveals that the normal 2- to 3-fold elevation of zinc concentration normally present in the hippocampal mossy fibers is absent in *Slc30a3* knockout (ZNT3) mice. Thus, the ZNT3 protein evidently controls not only the "stainability" but also the actual mass of zinc in mossy-fiber synaptic vesicles. This work thus confirms the metal-transporting role of the ZNT3 protein in the brain. **(J Histochem Cytochem 56:3–6, 2008)**

KEY WORDS
mossy fibers
ZNT3
glutamate
zinc release
hilus
X-ray
fluorescence
knockout

MORE THAN A DECADE AGO, Dr. Richard Palmiter discovered and cloned a gene (*Slc30a3*) the protein from which (ZNT3) he showed to be selectively located on the vesicles of zinc-secreting neurons, such as those comprising the hippocampal mossy-fiber pathway (Palmiter et al. 1996; Wenzel et al. 1997). Mice congenitally lacking the ZNT3 protein (ZNT3 knockout mice) were developed by Cole et al. (1999), and these mice proved to have no histochemically detectable zinc whatsoever in their mossy-fiber pathway, or in other zinc-secreting pathways (Cole et al. 1999); implying that the ZNT3 protein serves as a zinc transporter, responsible for the loading of zinc into those vesicles. The experiments performed by both Palmiter et al. (1996) and Cole et al. (1999) used immunocytochemistry to show that ZNT3 in the hippocampus is localized to the CA4/hilar region of the dentate gyrus, the stratum lucida of CA3, and the pyramidal cells of CA3 and CA1. Cole et al. (1999) also performed an elemental analysis of digested brain regions, demonstrating that total hippocampal zinc was reduced by 20%. The present work was undertaken to confirm that knocking out ZNT3 results in the loss of elemental zinc from the normally zinc-enriched regions of the hippocampus by using a novel non-destructive technique, microprobe synchrotron X-ray fluorescence (μSXRF).

The specific question under examination in the present work was, Does the ZNT3 protein control the amount of zinc stored in vesicles of zinc-secreting neurons, or does ZNT3 merely control the amount of zinc that is detectable by histochemical methods, i.e., control the speciation, or distribution between bound and free (rapidly exchangeable) zinc in the vesicle? The answer we have obtained by quantitative imaging of total elemental zinc, using μSXRF, in the hippocampal regions studied by Cole et al. (1999), of ZNT3 knockout mice and wild-type mice is unambiguous: mice lacking the ZNT3 protein have no detectable enrichment of elemental zinc in their vesicles. Moreover, there is even a suggestive diminution of zinc in the somata of the neurons that sequester large amounts of zinc in

Correspondence to: C.J. Frederickson, NeuroBioTex, Inc., 101 Christopher Columbus Blvd., Galveston, TX 77550. E-mail: c.j.frederickson@neurobiotex.com

Received for publication June 15, 2006; accepted July 18, 2007 [DOI: 10.1369/jhc.6A7035.2007].

 0022-1554/07/$3.30

their vesicles, the granule neurons of the dentate gyrus. μSXRF was used because it is a non-destructive technique that measures the total amount of metals present in a sample. This is a very useful technique in the case of zinc, because other fluorescence-based methods do not measure zinc that is bound in proteins. In μSXRF, incident X-ray radiation is absorbed by and re-emitted from the sample in an energy-dispersive spectrum in which the frequency of the fluorescent radiation depends on the binding energies of the metal. This method can be used to measure the metal concentrations at one point, or to determine the distribution across an area (using a movable stage). Because the incident X-ray beams have been collimated to smaller diameters, e.g., <10 μm, it has become possible to map the metal distribution in brain tissue from humans and animals (Collingwood et al. 2005; Flinn et al. 2005; Liu et al. 2006; Miller et al. 2006). By measuring the number of photons emitted at specific frequencies (13.5 keV for zinc), the relative concentrations of a metal can be determined in different samples (with detection limits of transition metals ranging from 0.1 to 5 ppm). To obtain absolute values, external standards must be used, as described below.

Materials and Methods

Animal care and experiments were performed in accordance with the Guidelines for Care and Use of Laboratory Animals (University of Ulsan, Seoul, South Korea). Two adult male mice lacking the *Slc30a3* gene, which encodes the ZNT3 protein, and two adult male wild-type mice were killed by an overdose of anesthetic. The brains were frozen in powdered dry ice, then cut with a cryostat microtome at a thickness of 20 μm and thawed onto silica (metal-free) slides. μSXRF was used to map the spatial distribution of zinc in the hippocampal formation of two sections from one knockout mouse and one wild-type mouse, and from one section in each of the other two mice. These were examined at beamline X26A of the National Synchrotron Light Source, Brookhaven National Laboratory. Bright-field pictures (20× objective) of unstained sections were also made for orientation and superposition on the μSXRF images. Spatial resolutions of 38 μm and 45 μm per inter-pixel step were used for the X-ray analysis, together with a 7-sec integration time per pixel.

The incident X-ray beam was tuned to 10 keV using an Si (111) channel-cut monochromator. This monochromatic beam was collimated to 350 μm in diameter using a set of tantalum slits and then focused to 10 μm in diameter using Rh-coated silicon microfocusing mirrors in Kirkpatrick-Baez–type geometry. Energy-dispersive X-ray fluorescence data were collected using a Canberra SL30165 Si (Li) detector. Regardless of resolution, each step is represented by a false-color pixel based on X-ray fluorescence intensity for the Zn Ka1 emission line.

For calibration of the X-ray fluorescence results, the standards were prepared using sheep brain neocortex, free of white matter and vascular content, which was then homogenized by ultrasonification. Aliquots were placed in Eppendorf tubes and the amount of tissue weighed. The samples were then diluted with zinc in solution, at concentrations of 1000, 500, or 250 ppm, to yield samples that contained 10, 20, 50, and 100 ppm more zinc than the original tissue. The samples were then frozen, thawed, and refrozen, because prior studies showed that this procedure yielded the most-uniform standards. A cryostat was used to cut 20-μm sections, which were placed onto zinc-free silica slides. These sections were then examined by μSXRF.

The linear-regression line through these points had an r^2 of 0.998, and the total zinc in the non-spiked, wet-brain homogenate was calculated using the method of standard additions (−1 * X intercept), to be 5.5 ppm, which, for a sample of 50% gray and 50% cortical white matter, would be a final concentration (dry weight) of 27.5 ppm for the gray (80% water) and 18 ppm for the white (70% water), or 23 ppm overall. Final ppm (dry) values for the mouse tissue samples were calculated from the regression line ($r^2 = 0.997$) of true total zinc (spike + endogenous zinc), according the formula ppm of zinc = 8.3 × counts.

Results

The difference between the knockout and wild-type mice was essentially all or none. Specifically, the wild-type mice had obvious focal enrichment of elemental zinc in mossy-fiber neuropil regions of the CA4-dentate hilar region, amounting to ∼2.5-fold enrichment over other, non–mossy-fiber regions, and the knockout mice did not have any such enrichment (Figure 1). In fact, the distribution of elemental zinc was so uniform in the images from the knockout mice that the pseudocolor image of zinc concentration showed no trace of the mossy-fiber neuropil. It was necessary to superimpose the bright-field images onto the pseudocolor images of the knockout mice for any boundaries to be evident in the cytoarchitecture (Figure 1). In all, both wild-type mice (2/2) had conspicuous zinc enrichment defining the hilar region and neither knockout mouse (0/2) had any detectable zinc enrichment there ($p<0.05$; $2 \times 2\ \chi^2$). Quantitatively, all three regions in the knockout mice had an average of between 71 and 74 ppm of zinc, i.e., no regional enrichment. The results differed by a maximum of ±1.5% between comparable areas from the two sections from the same mouse. In the two wild-type mice, the conspicuous enrichment of zinc in the hilar region (250 ppm) was ∼2.5-fold compared with the "background zinc" of the molecular zone of the dentate gyrus (95 ppm), and the granule cell stratum was intermediate (150 ppm). The values for the wild-type mice were somewhat higher than but in the same relative pattern as the established reference values for the rat hippocampal formation (Frederickson et al. 1983; Klitenick et al. 1983). Values between comparable areas from the two sections from the same mouse differed by at most ±11%. We also note that the conspicuous visible enrichment in total zinc in the mossy-fiber regions seen here in the two wild-type mice has

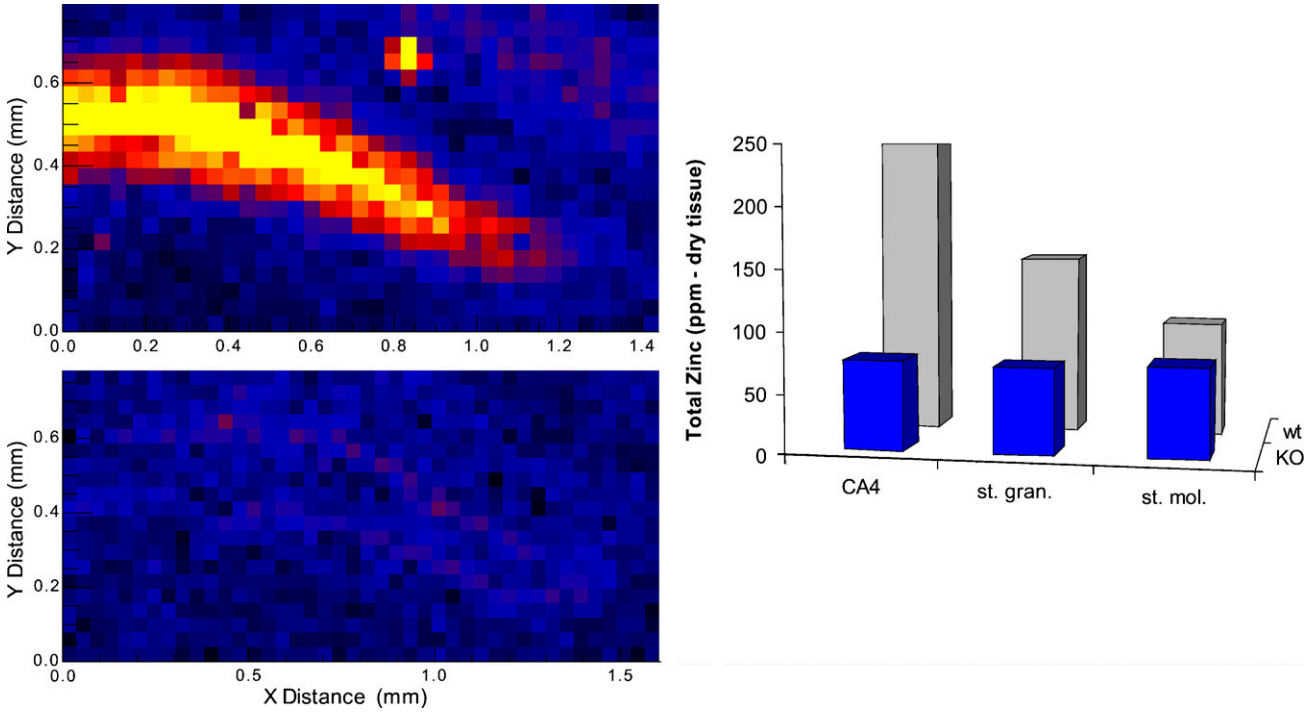

Figure 1 The total elemental zinc in the dentate gyrus region of ZNT3 knockout mice (KO) and wild type mice (wt) is shown in pseudocolor on the left for two mice, and in quantitative form in the histogram, which shows average values for the two knockout mice and the two wild-type mice (one section from each mouse) for the three regions indicated. (CA4, cornu ammonis 4; st. mol., stratum molecular; st. gran., stratum granular). With $n=2$ for each group, the absolute values of the ppm of zinc should be taken only as estimates.

been seen in 100% of the hilar–mossy-fiber regions of all of the mice ($n=4$) and rats ($n=4$) that we have examined by the X-ray fluorescence method in other ongoing studies (data not shown). The probability of observing the enrichment in all six normal mice (6/6) and none of the knockout mice (0/2) by chance is remote ($\chi^2 = 8$; $p<0.01$).

Discussion

The μSXRF technique used in this experiment has allowed for the quantification of total zinc in regions of the hippocampal formation and has confirmed more-traditional, non-quantitative histochemical findings measuring loosely bound or free zinc. In addition, μSXRF uses two-dimensional maps, which facilitated the comparison of specific hippocampal regions in the two types of mouse. The results demonstrate the efficacy of the ZNT3 knockout mouse, and confirm that the ZNT3 protein is an important neuronal zinc transporter. Indeed, one clear result of the present work is that the loss of the ZNT3 protein completely abolishes the selective enrichment of zinc in the cytoarchitecture of the mossy-fiber axons. This is consistent with immunocytochemical data already reported (Palmiter et al. 1996). Thus, the possibility that ZNT3 merely modulates "stainability" (i.e., speciation, or distribution among free and bound forms) of the zinc in the vesicles can be ruled out. The fact that the granule somata were also lower in zinc in the knockout mice than in the wild-type mice implies that the lack of ZNT3 depletes even the Golgi apparatus and perinuclear cytosol of zinc-secreting neurons, where the ZNT3 protein can normally be seen decorating the emerging vesicles (Cole et al. 1999). Because no brain region lacking zinc-secreting innervation (e.g., corpus callosum, cerebellum, brain stem) was measured in our work, we cannot say whether a lack of the ZNT3 protein affects any non-synaptic zinc pool, as has been suggested (Friedlich et al. 2004).

Why the ZNT3 knockout mice (which can now be said to lack any enrichment of zinc in their vesicles) do not show more behavioral and physiological differences from wild-type mice remains enigmatic, especially in view of all the evidence that synaptically released zinc is a potent modulator of brain function (Frederickson et al. 1990; Lassalle et al. 2000; Li et al. 2001,2003; Molnar and Nadler 2001). Cole et al. (2001) suggested that compensating mechanisms may play a role, and it is known that knockout mice do not always exhibit expected behavioral deficits (see, for example, Ste Marie et al. 2005; Agatsuma et al. 2006). However, these data indicate that reduced levels of zinc in the hilar region of the hippocampus do not affect the behaviors,

including spatial learning or sensorimotor function, examined by Cole et al. (2001).

Acknowledgments

This study was supported by a Brookhaven National Laboratory general user grant for National Synchrotron Light Source beamline access (JMF); and by Financial Assistance Award DE-FC09-96R18546 from the US Department of Energy (DOE) to the University of Georgia Research Foundation. The X26A microprobe beamline is supported in part by DOE grant DE-FG02-92ER14244. The National Synchrotron Light Source (NSLS) is supported by the US DOE under contract no. DEAC02-76CH00016. Support, in part, came also from National Institutes of Health Grants NS-41682, NS-42849, and EB-003924 to CJF.

We thank the NSLS staff for assistance.

Literature Cited

Agatsuma S, Lee M, Zhu H, Chen K, Shih JC, Seif I, Hiroi N (2006) Momoamine oxydase A knockout mice exhibit impaired nicotine preference but normal responses to novel stimuli. Hum Mol Genet 15:2721–2731

Cole TB, Martyanova A, Palmiter RD (2001) Removing zinc from synaptic vesicles does not impair spatial learning, memory, or sensorimotor functions in the mouse. Brain Res 891:253–265

Cole TB, Wenzel HJ, Kafer KE, Schwartzkroin PA, Palmiter RD (1999) Elimination of zinc from synaptic vesicles in the intact mouse brain by disruption of the ZnT3 gene. Proc Natl Acad Sci USA 96:1716–1721

Collingwood JF, Mikhaylova A, Davidson M, Batich C, Streit WJ, Terry J, Dobson J (2005) In situ characterization and mapping of iron compounds in Alzheimer's disease tissue. J Alzheimers Dis 7:267–272

Flinn JM, Hunter D, Linkous DH, Lanzirotti A, Smith LN, Brightwell J, Jones BF (2005) Enhanced zinc consumption causes memory deficits and increased brain levels of zinc. Physiol Behav 83:793–803

Frederickson CJ, Klitenick MA, Manton WI, Kirkpatrick JB (1983) Cytoarchitectonic distribution of zinc in the hippocampus of man and the rat. Brain Res 273:335–339

Frederickson RE, Frederickson CJ, Danscher G (1990) In situ binding of bouton zinc reversibly disrupts performance on a spatial memory task. Behav Brain Res 38:25–33

Friedlich AL, Lee JY, Van GT, Cherny RA, Volitakis I, Cole TB, Palmiter RD, et al. (2004) Neuronal zinc exchange with the blood vessel wall promotes cerebral amyloid angiopathy in an animal model of Alzheimer's disease. J Neurosci 24:3453–3459

Klitenick MA, Frederickson CJ, Manton WI (1983) Acid-vapor decomposition for determination of zinc in brain tissue by isotope dilution mass spectrometry. Anal Chem 55:921–923

Lassalle JM, Bataille T, Halley H (2000) Reversible inactivation of the hippocampal mossy fiber synapses in mice impairs spatial learning, but neither consolidation nor memory retrieval, in the Morris navigation task. Neurobiol Learn Mem 73:243–257

Li Y, Hough CJ, Frederickson CJ, Sarvey JM (2001) Induction of mossy fiber –> Ca3 long-term potentiation requires translocation of synaptically released Zn2+. J Neurosci 21:8015–8025

Li YV, Hough CJ, Sarvey JM (2003) Do we need zinc to think? Sci STKE 182:pe19

Liu G, Huang W, Moir RD, Vanderburg CR, Lai B, Peng Z, Tanzi RE, et al. (2006) Metal exposure and Alzheimer's pathogenesis. J Struct Biol 155:45–51

Miller LM, Wang Q, Telivala TP, Smith RJ, Lanzirotti A, Miklossy J (2006) Synchrotron-based infrared and X-ray imaging shows focalized accumulation of Cu and Zn co-localized with beta-amyloid deposits in Alzheimer's disease. J Struct Biol 155:30–37

Molnar P, Nadler JV (2001) Synaptically-released zinc inhibits N-methyl-D-aspartate receptor activation at recurrent mossy fiber synapses. Brain Res 910:205–207

Palmiter RD, Cole TB, Quaife CJ, Findley SO (1996) ZNT3, a putative transporter of zinc into synaptic vesicles. Proc Natl Acad Sci USA 93:14934–14939

Ste Marie L, Luquet S, Cole TB, Palmiter RD (2005) Modulation of neuropeptide Y expression in adult mice does not affect feeding. Proc Natl Acad Sci USA 102:18632–18637

Wenzel HJ, Cole TB, Born DE, Schwartzkroin PA, Palmiter RD (1997) Ultrastructural localization of zinc transporter-3 (ZNT3) to synaptic vesicle membranes within mossy-fiber boutons in the hippocampus of mouse and monkey. Proc Natl Acad Sci USA 94: 12676–12681